favored, with the second ligand being incorporated with formation constants of 1.7 and 17 M^{-1}, respectively, for the above two systems. Apparently there is a weak synergistic effect accompanying the change in coordination geometry.

In contrast to the above reactions, vanadate condenses in an almost stoichiometric manner with the 2-pyridinecarboxylates, picolinate and 3-hydroxypicolinate. The formation of the mono(ligand) product proceeds with an equilibrium constant of approximately 150 M^{-1}. Thus, these products are favored by about 3 orders of magnitude over those formed with the hydroxy acids.

On the basis of the positions of the ^{51}V chemical shifts, there may be a change in coordination geometry upon going to the bis(ligand) derivatives from the mono products. The bis products have equilibrium constants ranging from about 200 to 700 M^{-1} for the formation of the bis products from the mono derivatives.

Of some interest in the 3-hydroxypicolinate system is the condensation of vanadate between the carboxy and hydroxy groups to form products that are analogous to those formed from salicylate and 2-hydroxynicotinate. An intense signal at a ^{51}V chemical shift of −536 ppm is observed, and this is close in frequency to the signals from the above products, i.e. approximately −534 ppm. However, the formation constant for this product is about 4 orders of magnitude larger than those observed for the salicylate and 2-hydroxynicotinate ligands. As a consequence, if this product is in fact formed with the hydroxy/carboxylate groups of the pyridine ring, then it seems that product formation is strongly promoted by protonation at the nitrogen to form a pyridinium adduct. The possibility that this derivative is simply a product of reaction at the nitrogen and carboxylate functionalities cannot be ruled out.

Contribution from the Departments of Chemistry, University of Denver, Denver, Colorado 80208, and University of Colorado at Denver, Denver, Colorado 80204, and Central Laboratory of Chemistry, University of Pecs, 7643 Pecs, Hungary

Metal–Nitroxyl Interactions. 53. Effect of the Metal–Nitroxyl Linkage on the Electron–Electron Exchange Interaction in Spin-Labeled Complexes of Copper(II), Low-Spin Cobalt(II), Vanadyl, and Chromium(III)

Kundalika M. More, Gareth R. Eaton,* Sandra S. Eaton, Olga H. Hankovszky, and Kálmán Hideg

To examine the effect of several metal–nitroxyl linkages on the magnitude of the electron–electron interaction, EPR spectra were obtained for two spin-labeled isoquinolines and nine spin-labeled pyridines bound to copper(II) bis(hexafluoroacetylacetonate), cobalt(II) tetrakis(*p*-(trifluoromethyl)phenyl)porphyrin, vanadyl bis(hexafluoroacetylacetonate), and chromium(III) tetraphenylporphyrin chloride. The Cu(II) and vanadyl complexes were studied in fluid solution and frozen solution, and the Co(II) and Cr(III) complexes were studied in frozen solution. The values of the metal–nitroxyl electron–electron coupling constant, *J*, for the isoquinoline complexes were about a factor of 10 smaller than for complexes of spin-labeled pyridines with the same linkage between the heterocyclic ring and the nitroxyl. The differences in the value of *J* for isomers of the same ligand indicated that the value of *J* is strongly dependent on the conformation of the pyridine–nitroxyl linkage. Addition of a carbonyl group to the metal–nitroxyl linkage caused the value of *J* to decrease by a factor of 10–70. When the 2-isomer could not form a chelate ring, the value of *J* for the copper complex of the 2-isomer was about twice as large as for the 4-isomer. A saturated (CH$_2$)$_2$ linkage to the 2-carbon of the nitroxyl ring resulted in about the same strength of exchange interaction as an unsaturated (CH=CH) linkage to the 3-carbon. When the pyridine was attached directly to the 2-carbon of the nitroxyl ring, the exchange interaction was sufficiently large that only a lower limit on the value of *J* was obtained. The barrier to rotation about a single bond in four of the ligands was about 5 kcal/mol.

Introduction

Electron–electron spin–spin interaction reflects the extent of electron spin delocalization. If the strength of the interaction is of the same order of magnitude as the separation between the electron-spin energy levels, it can be measured by EPR.[1,2] These interactions frequently can be observed through as many as 8 to 12 bonds. The interaction is strongly dependent on the number of atoms in the linkage between the two paramagnetic centers, the conformation of the linkage, and the σ and π contributions to the bonding. The data currently available are not sufficient to predict the magnitude of spin–spin interaction from a knowledge of the linkage between the two paramagnetic centers. We are therefore exploring the effect of the linkage between a paramagnetic metal and a nitroxyl radical on the electron–electron spin–spin interaction.[3]
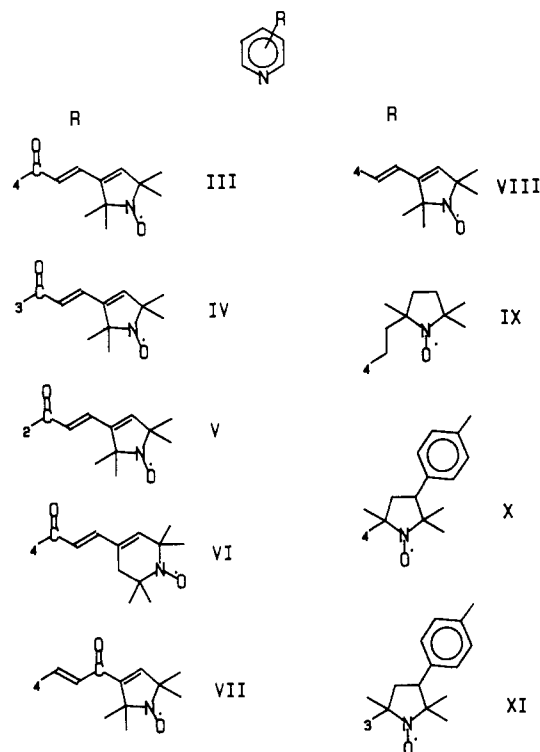
The ligands in this study were selected to examine several questions concerning electron spin delocalization. Spin-labeled isoquinolines I and II permit comparison with previously reported data on analogous spin-labeled pyridines.[3-5] Spin-labeled pyridines III–VIII permit assessment of the impact of addition of a carbonyl
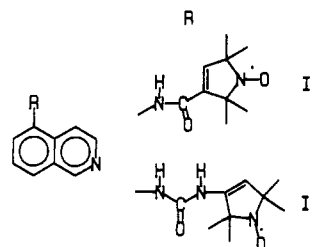
group to the metal–nitroxyl linkage, the impact of moving the substituent between positions on the pyridine ring, and the effect of changing the size of the nitroxyl ring. Spin-labeled pyridines IX–XI were selected because the metal–nitroxyl linkage is through the 2-carbon of the nitroxyl ring rather than the 3-carbon or 4-carbon as in III–VIII.

---

(1) Eaton, G. R.; Eaton, S. S. *Acc. Chem. Res.* **1988**, *21*, 107.
(2) Eaton, S. S.; Eaton, G. R. *Spin Labeling III*; Berliner, L. J., Ed.; Plenum: New York, 1989.
(3) Eaton, S. S.; Eaton, G. R. *Coord. Chem. Rev.* **1988**, *83*, 29.
(4) Sawant, B. M.; Shroyer, A. L. W.; Eaton, G. R.; Eaton, S. S. *Inorg. Chem.* **1982**, *21*, 1093.
(5) More, J. K.; More, K. M.; Eaton, G. R.; Eaton, S. S. *Inorg. Chem.* **1982**, *21*, 2455.

---

*To whom correspondence should be addressed at the University of Denver.

III IV V VI VII VIII IX X XI

Scheme I

4-Py ; III
3-Py ; IV
2-Py ; V

VI

VII

VIII

XII XIII IX

XIV

Complexes of I–XI with copper(II) bis(hexafluoroacetylacetonate) (Cu(hfac)$_2$), cobalt(II) tetrakis(p-(trifluoromethyl)-phenyl)porphyrin (Co(P)), vanadyl bis(hexafluoroacetylacetonate) (VO(hfac)$_2$), and chromium(III) tetraphenylporphyrin chloride (Cr(TPP)Cl) were studied. Each of these metal complexes forms a 1:1 complex with pyridine. The Cu(hfac)$_2$, Co(P), and VO-(hfac)$_2$ complexes have one metal unpaired electron ($S = {}^1/_2$), but Cr(TPP)Cl has three unpaired electrons ($S = {}^3/_2$). The symmetry of the metal orbitals containing the unpaired electron(s) with respect to the orbitals on the coordinated nitrogen is σ for Cu(hfac)$_2$ and Co(P) and π for VO(hfac)$_2$ and Cr(TPP)Cl.

Experimental Section

Physical Measurements. Infrared spectra were obtained in Nujol mulls on a Perkin-Elmer 283B spectrometer for ligands I and II. Infrared spectra of ligands III–XI were run in KBr pellets on a Bruker IFS-113v vacuum optic FT spectrometer equipped with an Aspect 2000 computer or as Nujol mulls on a Zeiss Specord 75 spectrometer. Melting points were determined by using a Buchi micro melting-point apparatus and are uncorrected.

^{1}H NMR spectra were recorded at 200 or 250 MHz on Bruker spectrometers, and ^{13}C NMR spectra were obtained at 20.14 MHz on a Bruker WP.80SY spectrometer with proton decoupling. The spectrometers were locked on the deuterium signal from the CDCl$_3$ solvent, and TMS was the internal reference. Diphenylhydrazine was used to reduce the nitroxyl radicals to obtain the NMR spectra.[6] The pyridine resonances in the ^{13}C NMR spectra of III, IV, and VIII were tentatively assigned by calculating the expected substituent effects with use of the equations in ref 7.

X-Band EPR spectra were obtained on a Varian E9 instrument interfaced to an IBM CS9000[8] data station or on an IBM ER200 instrument with an IBM CS9000. Spectra were obtained with 100-kHz modulation at modulation amplitudes that did not distort the line shapes and microwave powers that did not cause saturation. Q-Band EPR spectra were obtained on a spectrometer that has been described previously.[9] The solutions used to obtain the spectra contained approximately equimolar metal complex and spin-labeled ligand at $(1-2) \times 10^{-3}$ M. The lines in the spectra were sufficiently broad that degassing the solutions
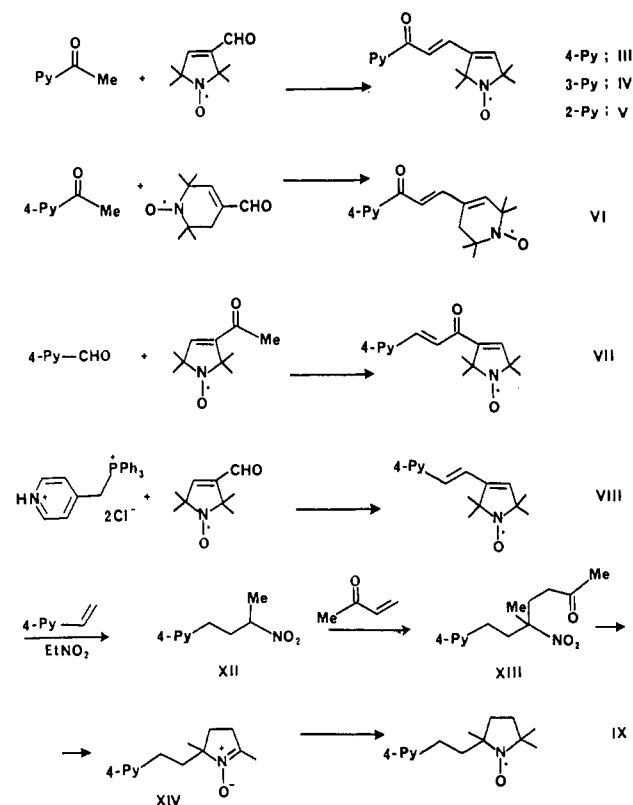
did not alter the spectra, so spectra were obtained on air-saturated solutions for complexes of Cu(hfac)$_2$, VO(hfac)$_2$, and Cr(TPP)Cl. For the Co(P) complexes, solutions were prepared in the absence of oxygen to prevent the formation of Co(P)·L(O$_2$).

Preparation of Compounds. The following compounds were prepared by literature methods: V,[6] Cu(hfac)$_2$,[10] VO(hfac)$_2$,[11] Co(P),[12] and Cr-(TPP)Cl.[13]

5-(((2,2,5,5-Tetramethyl-1-oxypyrrolin-3-yl)carbonyl)amino)iso-quinoline (I). To the acid chloride of 2,2,5,5-tetramethyl-1-oxy-pyrroline-3-carboxylic acid[14] (0.405 g, 2.0 mmol) in dry THF (50 mL) was added pyridine (2 mL) and 5-aminoisoquinoline (0.288 g, 2.0 mmol). After the reaction mixture was refluxed overnight, the solvent was removed under vacuum. The residue was dissolved in chloroform (75 mL), and the solution was washed several times with 0.1 M NaOH solution (total volume ca. 200 mL), washed once with water, and dried over anhydrous Na$_2$SO$_4$. The solvent was removed under vacuum. The residue was dissolved in a minimum volume of CHCl$_3$ and put on a silica gel column. After elution of impurities with CHCl$_3$, the product was eluted with 2% MeOH in CHCl$_3$ as a slow-moving yellow band. The solvent was removed under vacuum, and the product was recrystallized from benzene–hexane: yield 0.15 g, 24%; mp 174 °C. IR: 1620 (C=C), 1670 (C=O), 3220 (NH) cm^{-1}. Anal. Calcd for C$_{18}$H$_{20}$N$_3$O$_2$: C, 69.66; H, 6.50; N, 13.54. Found: C, 69.68; H, 6.56; N, 13.62.

5-((((2,2,5,5-Tetramethyl-1-oxypyrrolin-3-yl)amino)carbonyl)-amino)isoquinoline (II). 3-Isocyanato-2,2,5,5-tetramethylpyrrolinyl-1-oxy[15] (0.183 g, 1.0 mmol) was added to a solution of 5-aminoisoquinoline (0.144 g, 1.0 mmol) in THF (50 mL). After the solution was refluxed overnight, the solvent was removed under vacuum. The residue was dissolved in CHCl$_3$, and the solution was chromatographed on a silica gel column. Impurities were eluted with CHCl$_3$, and the product was eluted as a slow-moving yellow band with 2% MeOH in CHCl$_3$. After

(6) Hankovszky, H. O.; Hideg, K.; Lex, L.; Kulcsár, Gy.; Halász, H. A. *Can. J. Chem.* **1982**, *60*, 1432.

(7) Kalinowski, H.-O.; Berger, S.; Braun, S. *Carbon-13 NMR Spectroscopy*; Wiley: Chicester, England, 1988; pp 400–401 (English translation).

(8) Quine, R. W.; Eaton, G. R.; Eaton, S. S. *J. Magn. Reson.* **1986**, *66*, 164.

(9) Eaton, S. S.; More, K. M.; DuBois, D. L.; Boymel, P. M.; Eaton, G. R. *J. Magn. Reson.* **1980**, *41*, 150.

(10) Funck, L. L.; Ortolano, T. R. *Inorg. Chem.* **1968**, *7*, 567.

(11) Su, C.; Reed, J. W.; Gould, E. S. *Inorg. Chem.* **1973**, *12*, 337. Drago, R. S.; Kuechler, T. C.; Kroeger, M. *Inorg. Chem.* **1979**, *18*, 2337.

(12) Eaton, S. S.; Boymel, P. M.; Sawant, B. M.; More, J. K.; Eaton, G. R. *J. Magn. Reson.* **1984**, *56*, 183.

(13) Summerville, D. A.; Jones, R. D.; Hoffman, B. M.; Basolo, F. *J. Am. Chem. Soc.* **1977**, *99*, 8195.

(14) Rozentsev, E. G. *Free Nitroxyl Radicals*; Hazzard, B. J., Translator; Plenum Press: New York, 1970; p 209.

(15) DuBois, D. L.; Eaton, G. R.; Eaton, S. S. *J. Am. Chem. Soc.* **1978**, *100*, 2686. Hankovszky, H. O.; Hideg, K.; Tigyi, J. *Acta Chim. Acad. Sci. Hung.* **1978**, *98*, 339.

removal of the solvent under vacuum, the product was recrystallized from CH$_2$Cl$_2$–hexane: yield 0.25 g, 77%; mp 188 °C. IR: 1720 (C=O), 3320 (NH) cm^{-1}. Anal. Calcd for C$_{18}$H$_{21}$N$_4$O$_2$: C, 66.44; H, 6.51; N, 17.22. Found: C, 66.33; H, 6.58; N, 17.17.

The synthesis of ligands III–IX are outlined in Scheme I and are described in detail below.

Preparation of III–V. To a stirred ice-cold solution of 2,2,5,5-tetramethyl-3-formylpyrrolinyl-1-oxy[16] (0.168 g, 1.0 mmol) and an acetylpyridine (0.121 g, 1.0 mmol) in 5 mL of MeOH was added a 10% aqueous solution of sodium hydroxide (0.5 mL, 1.1 mmol). The precipitation of the yellow product was completed by adding water. The crude material was crystallized from chloroform–hexane.

1-(4-Pyridyl)-3-(2,2,5,5-tetramethyl-1-oxypyrrolin-3-yl)propenone (III). Yield: 0.180 g, 66%. MP: 157–158 °C. IR: 1668 (C=O) cm^{-1}. ^{1}H NMR (ppm): 1.27, 1.39 (2 s, 12 H, 4 CH$_3$); 6.10 (s, 1 H, CH=, pyrroline); 7.01, 7.31 (2 d, 2 H, J = 16.0 Hz, CH=CH); 7.64 (d, 2 H, J = 6 Hz, py 3,5-H); 8.76 (d, 2 H, J = 6 Hz, py 2,6-H). ^{13}C NMR (ppm): 25.0, 25.3, 67.7, 69.5 (4 CH$_3$); 121.4 (py 3,5-C); 121.9, 140.3, 141.8, 144.3 (4 olefinic C); 143.0 (py 4-C); 150.6 (py 2,6-C); 189.7 (CO). Anal. Calcd for C$_{16}$H$_{19}$N$_2$O$_2$: C, 70.85; H, 7.06; N, 10.32. Found: C, 70.84; H, 7.05; N, 10.31.

1-(3-Pyridyl)-3-(2,2,5,5-tetramethyl-1-oxypyrrolin-3-yl)propenone (IV). Yield: 0.170 g, 63%. Mp: 125–126 °C. IR: 1664 (C=O) cm^{-1}. ^{1}H NMR (ppm): 1.28, 1.40 (2 s, 12 H, 4 CH$_3$); 6.11 (s, 1 H, CH= pyrroline); 7.10, 7.33 (2 d, 2 H, J = 16.0 Hz, CH=CH); 7.3 (m, 1 H, py 5-H); 8.2 (d, 1 H, py 4-H); 8.75 (d, 1 H, py 6-H); 9.15 (s, 1 H, py 2-H). ^{13}C NMR (ppm): 24.9, 25.2, 68.0, 69.8 (4 CH$_3$); 122.1 (py 5-C); 123.7, 139.5, 141.7, 142.1 (4 olefinic C); 133.3 (py 3-C); 135.9 (py 4-C); 149.5, 152.9 (py 2,6-C); 188.8 (CO). Anal. Calcd for C$_{16}$H$_{19}$N$_2$O$_2$: C, 70.85; H, 7.06; N, 10.32. Found: C, 70.65; H, 7.16; N, 10.34.

1-(4-Pyridyl)-3-(2,2,6,6-tetramethyl-1,2,5,6-tetrahydro-1-oxypyridin-4-yl)propenone (VI). 4-Acetylpyridine (0.121 g, 1.0 mmol) and 2,2,6,6-tetramethyl-4-formyl-1,2,5,6-tetrahydropyridinyl-1-oxy[17] (0.170 g, 1.0 mmol) were condensed as described above for the preparation of III–V: yield 0.186 g, 65%; mp 141–142 °C. ^{1}H NMR (ppm): 1.23, 1.30 (2 s, 12 H, 4 CH$_3$); 2.30 (s, 2 H, nitroxyl ring CH$_2$); 6.02 (s, 1 H, nitroxyl ring =CH); 6.72, 7.42 (2 d, 2 H, J = 16.0 Hz, CH=CH); 7.7 (d, 2 H, py 3,5-H); 8.8 (d, 2 H, py 2,6-H). Anal. Calcd for C$_{17}$H$_{21}$N$_2$O$_2$: C, 71.55; H, 7.42; N, 9.82. Found: C, 71.52; H, 7.39; N, 10.01.

1-(2,2,5,5-Tetramethyl-1-oxypyrrolin-3-yl)-3-(4-pyridyl)propenone (VII). A solution of 2,2,5,5-tetramethyl-3-acetylpyrrolinyl-1-oxy[6,18] (0.182 g, 1.0 mmol) and 4-formylpyridine (0.107 g, 1.0 mmol) in 5 mL of MeOH was treated with 10% sodium hydroxide solution as described above for the preparation of III–V. The reaction led to a mixture of products, so the crude product was flash chromatographed on silica gel. The first band eluted with 1% MeOH in CHCl$_3$ was the desired product: yield 0.200 g, 74%; mp 130–132 °C. IR: 1660 (C=O) cm^{-1}. Anal. Calcd for C$_{16}$H$_{19}$N$_2$O$_2$: C, 70.85; H, 7.06; N, 10.32. Found: C, 70.83; H, 7.19; N, 10.21.

1-(2,2,5,5-Tetramethyl-1-oxypyrrolin-3-yl)-2-(4-pyridyl)ethylene (VIII). A solution of 4-(chloromethyl)pyridine hydrochloride (1.64 g, 0.01 mol) and triphenylphosphine (2.62 g, 0.01 mol) in dimethylformamide (25 mL) was heated at 75 °C for 2 h and evaporated in vacuo, and the residue was cooled and diluted with acetone–ether to precipitate the phosphonium salt. The pink solid was collected by filtration: yield 3.50 g, 82%; mp >250 °C. Anal. Calcd for C$_{24}$H$_{22}$Cl$_2$NP: C, 67.61; H, 5.20; N, 3.29. Found: C, 67.53; H, 5.28; N, 3.32.

To a stirred solution of this phosphonium salt (2.13 g, 5.0 mmol) and 2,2,5,5-tetramethyl-3-formylpyrrolinyl-1-oxy[16] (0.84 g, 5.0 mmol) in dioxane (10 mL) and water (10 mL) was added K$_2$CO$_3$ (0.500 g), and the mixture was heated for 3 h. The reaction mixture was diluted with ether (20 mL). The organic phase was separated, dried over MgSO$_4$, and evaporated to dryness. The product (VIII) was crystallized from chloroform–hexane: yield 1.05 g, 86%; mp 98–99 °C. ^{1}H NMR (ppm): 1.28, 1.39 (2 s, 12 H, 4 CH$_3$); 5.83 (s, 1 H, CH=, pyrroline); 6.65, 6.75 (2 d, 2 H, J = 16.6 Hz, CH=CH); 7.25 (d, 2 H, py 3,5-H); 8.52 (d, 2 H, py 2,6-H). ^{13}C NMR (ppm): 25.1, 25.6, 67.4, 69.8 (4 CH$_3$); 120.6 (py 3,5-C); 126.8, 127.0, 135.1, 144.7 (4 olefinic C); 142.1 (py 4-C); 149.9 (py 2,6-C). Anal. Calcd for C$_{15}$H$_{19}$N$_2$O: C, 74.04; H, 7.87; N, 11.51. Found: C, 74.29; H, 7.78; N, 11.49.

3-Nitro-1-(4-pyridyl)butane (XII). To a solution of 4-vinylpyridine (4.21 g, 0.04 mol) and nitroethane (6.01 g, 0.08 mol) in dry tetrahydrofuran (20 mL) was added tetramethylguanidine (1 g) catalyst, and the solution was refluxed for 8 h. The solution was diluted with ether

(20 mL), washed with saturated aqueous NaCl and then with water, dried over MgSO$_4$, and evaporated to dryness. The residue was distilled as a colorless oil at 124–127 °C (0.6 mmHg); yield 3.75 g, 52%. (This compound was prepared previously[19] in MeOH solution with sodium methoxide as catalyst in 34% yield.) ^{1}H NMR (ppm): 1.55 (d, 3 H, J = 6.6 Hz, CH$_3$); 1.7–3.0 (m, 4 H, 2 CH$_2$); 4.2–4.9 (m, 1 H, CH); 7.07, 8.47 (2 d, 4 H, py 2,3,5,6-H).

5-Methyl-5-nitro-7-(4-pyridyl)heptan-2-one (XIII). A solution of XII (3.6 g, 0.02 mol) and methyl vinyl ketone (1.40 g, 0.02 mol) in dry ether (50 mL) was refluxed in the presence of 1,8-diazabicyclo[5.4.0]undec-7-ene (1.52 g, 0.01 mol) for 3 h and then washed with water. The ether layer was dried over MgSO$_4$, and the ether was removed. The product was purified by fractional distillation at 198–200 °C (0.1 mmHg); yield 2.65 g, 53%. IR: 1530, 1350 (NO$_2$); 1720 (C=O) cm^{-1}. Anal. Calcd for C$_{13}$H$_{18}$N$_2$O$_3$: C, 62.38; H, 7.25; N, 11.19. Found: C, 62.44; H, 7.12; N, 11.23.

2,5-Dimethyl-5-(2-(4-pyridyl)ethyl)pyrroline 1-Oxide (XIV). To a stirred solution of the γ-nitro ketone XIII (2.50 g, 0.01 mol) in MeOH (30 mL) and 10 mL of saturated NH$_4$Cl solution was added Zn powder (2.0 g) over 20 min at room temperature. After the mixture was stirred at room temperature for an additional 2 h, the inorganics were filtered off and washed with MeOH. The combined MeOH filtrates were evaporated to dryness. The residue was dissolved in CHCl$_3$, and the solution was dried over MgSO$_4$ and taken to dryness. The nitrone was chromatographed on silica gel by using 10% MeOH in CHCl$_3$ as eluent. The pure nitrone was obtained as a pale yellow oil; yield 1.27 g, 58%. IR: 1610 (C=N) cm^{-1}. Anal. Calcd for C$_{13}$H$_{18}$N$_2$O: C, 71.53; H, 8.31; N, 12.83. Found: C, 71.55; H, 8.19; N, 12.90.

2,5,5-Trimethyl-2-(2-(4-pyridyl)ethyl)-1-oxypyrrolidine (IX). To a stirred ether (20 mL) solution of methylmagnesium iodide (6.0 mmol; freshly prepared from methyl iodide (0.85 g, 6.0 mmol) and Mg (0.14 g, 6.0 mmol)) was added a solution of the nitrone XIV (1.09 g, 5.0 mmol) in dry ether (20 mL). After the mixture stood overnight at room temperature, the complex was decomposed with a saturated aqueous solution of NH$_4$Cl (10 mL). The ether phase was separated, dried over MgSO$_4$, and aerated in the presence of PbO$_2$ for 15 min. The solution was filtered, and the filtrate was evaporated to dryness. The yellow semisolid residue was chromatographed on silica gel and eluted with 10% MeOH in CCl$_4$: yield 0.873 g, 75%; mp 54–55 °C. Anal. Calcd for C$_{14}$H$_{21}$N$_2$O: C, 72.07; H, 9.07; N, 12.01. Found: C, 71.94; H, 9.11; H, 12.14.

The synthesis of ligands X and XI will be described elsewhere, in conjunction with the preparation of related nitroxyl radicals.[20]

Computer Simulations. The fluid-solution EPR spectra of Cu(hfac)$_2$·L and VO(hfac)$_2$·L were simulated with the computer program CUNO.[4,21] The parameters for the paramagnetic centers were as follows: Cu(II), g = 2.147 ± 0.002, A_{Cu} = 52 ± 1 G (0.0052 cm^{-1}); vanadyl, g = 1.970 ± 0.002, A_V = 108.0 ± 0.5 G (0.009 95 cm^{-1}); nitroxyl g = 2.0059, A_N = 14.2–15.7 G, depending on the nitroxyl ring. The frozen-solution spectra of the complexes with metal S = $^1/_2$ were simulated with the computer program MENO.[22] The parameters for the paramagnetic centers were as follows: Cu(II), g_x = 2.040, g_y = 2.107, g_z = 2.302, A_x = A_y = 0.0010 cm^{-1}, A_z = 0.0145 cm^{-1}; vanadyl, g_x = g_y = 1.984, g_z = 1.943, A_x = A_y = 0.0065 cm^{-1}, A_z = 0.0168 cm^{-1}; cobalt, g_x = g_y = 2.322–2.326, g_z = 2.027–2.031, A_x = A_y = 0.0005 cm^{-1}, A_z = 0.0082 cm^{-1}; nitroxyl, g_x = 2.0089, g_y = 2.0066, g_z = 2.0025, A_x = 0.0004 cm^{-1}, A_y = 0.0005 cm^{-1}, A_z = 0.0032–0.0036 cm^{-1}. The frozen-solution EPR spectra of Cr(TPP)Cl·L were simulated with the computer program METNO.[23] The parameters for Cr(III) were g = 1.996, D = 0.16 ± 0.005, and E = 0.013 ± 0.003 cm^{-1}. This program does not include the effects of the nitroxyl nitrogen nuclear spin, so calculations are limited to cases in which the spin–spin interaction is greater than the nitrogen nuclear hyperfine splitting.

Results and Discussion

For slowly relaxing paramagnetic centers, electron–electron spin–spin coupling that is greater than the line widths in the EPR spectra gives rise to AB patterns.[1] The relaxation time requirements are satisfied for Cu(hfac)$_2$·L and VO(hfac)$_2$·L at room temperature and –180 °C and for Co(P)·L and Cr(TPP)Cl·L at –180 °C. Therefore, the EPR spectra of the Cu(II) and vanadyl

(16) Hideg, K.; Hankovszky, H. O.; Lex, L.; Kulcsár, Gy. *Synthesis* **1980**, 911.

(17) Cseko, J.; Hankovszky, H. O.; Hideg, K. *Can. J. Chem.* **1985**, *63*, 940.

(18) Keana, J. F. W.; Hideg, K.; Birrell, G. B.; Hankovszky, H. O.; Ferguson, G. B.; Parvez, M. *Can. J. Chem.* **1982**, *60*, 1439.

(19) Profft, E. *Chem. Technol.* **1956**, *8*, 705.

(20) Hideg, K.; et al. To be submitted for publication.

(21) Eaton, S. S.; DuBois, D. L.; Eaton, G. R. *J. Magn. Reson.* **1978**, *32*, 251.

(22) Eaton, S. S.; More, K. M.; Sawant, B. M.; Boymel, P. M.; Eaton, G. R. *J. Magn. Reson.* **1983**, *52*, 435.

(23) More, K. M.; Eaton, G. R.; Eaton, S. S.; Hideg, K. *Inorg. Chem.* **1986**, *25*, 3865.

complexes of ligands I–XI were studied in fluid solution at room temperature and in frozen solution at –180 °C and the Co(II) and Cr(III) complexes of these ligands were studied in frozen solution at –180 °C. The analysis of AB patterns in EPR spectra has been reviewed.[1,2] For small molecules that are tumbling rapidly in fluid solution, anisotropic contributions to the spin–spin splitting are averaged out and only the isotropic exchange coupling is observed. The isotropic coupling constant is denoted as J. In frozen solution the spin–spin splitting includes the anisotropic dipolar contribution as well as the isotropic exchange contribution. For most of the ligands used in this study the interspin distance was >10 Å and the exchange term was the dominant contribution to the spin–spin interaction. As a result little information was obtained concerning the dipolar interaction. The values of J are summarized in Table I, in order of increasing strength of the exchange interaction. Selected spectra are discussed in the following paragraphs.

Olefin Conformations. ^{1}H and ^{13}C NMR spectra were analyzed to determine the geometry of the olefinic linkages in the reduced (diamagnetic) forms of III, IV, VI, and VIII. The proton spectra showed AB patterns with J = 16 Hz, which is consistent with a trans conformation. No peaks characteristic of the cis isomer were observed. In the ^{13}C spectra the number of signals indicated the presence of a single isomer. Apparently the reactions to form these ligands occur with sufficient stereoselectivity that the populations of the cis isomers are too small to be observed in the NMR spectra.

Copper Complexes. In equimolar solutions of ligand and Cu-(hfac)$_2$, the predominant species is the 1:1 complex, Cu(hfac)$_2$·L.[24] There is a small amount of dimer formation, in which a pyridine nitrogen is bound to one Cu(hfac)$_2$ and the nitroxyl oxygen of the same ligand is bound to a second Cu(hfac)$_2$. When the nitroxyl oxygen is bound to Cu(II), the antiferromagnetic interaction is sufficiently strong that an EPR signal is not observed. Thus, the EPR spectrum for the dimer is due only to the Cu(II) bound to the pyridine nitrogen, which is readily distinguished from the spectrum due to copper–nitroxyl interaction in Cu(hfac)$_2$·L.[24]

The exchange interactions for Cu(hfac)$_2$·L, L = VIII–XI, were stronger than for the other spin-labeled ligands included in this study. The fluid-solution X-band spectra of these complexes had signals at the average of the nitroxyl and copper g values, with copper hyperfine splitting that was half that observed in the absence of electron–electron spin–spin interaction. These spectra are characteristic of exchange interaction that is larger than the separation between the metal and nitroxyl electron-spin energy levels. The outer lines of the AB pattern have negligible intensity, and the metal and nitroxyl inner lines are equivalent. Only a lower limit on the value of J can be obtained from these spectra. Since the resonant magnetic field at Q-band is about 4 times that at X-band, the separation between the metal and nitroxyl energy levels that is due to g-value differences is 4 times greater at Q-band than at X-band. For some complexes that give averaged signals at X-band, it is possible to observe separate metal and nitroxyl inner lines in Q-band spectra and to obtain a value of J by simulation of the spectra.[1,25]

The Q-band spectrum of Cu(hfac)$_2$·VIII in toluene solution is shown in Figure 1A. The peaks labeled a and b are the copper and nitroxyl inner lines, respectively, of an AB pattern with J = 0.18 cm^{-1}. The copper and nitroxyl outer lines for this AB pattern occur at lower and higher fields, respectively, than are displayed in this 2000-G scan. Peaks c and f are the nitroxyl inner and outer lines of an AB pattern with J = 0.075 cm^{-1}. The ratio of the populations of the components with J = 0.18 and 0.075 cm^{-1} is about 5:1. The sharp triplet between peaks c and d is the nitroxyl signal for VIII that is not bound to Cu(hfac)$_2$. Peaks d and e are nitroxyl outer lines due to two AB patterns with J about 0.030 and 0.045 cm^{-1}, respectively. Since the intensity of the outer lines falls off rapidly as the value of J increases, the weak intensities of peaks d and e compared with that of peak f indicate that the
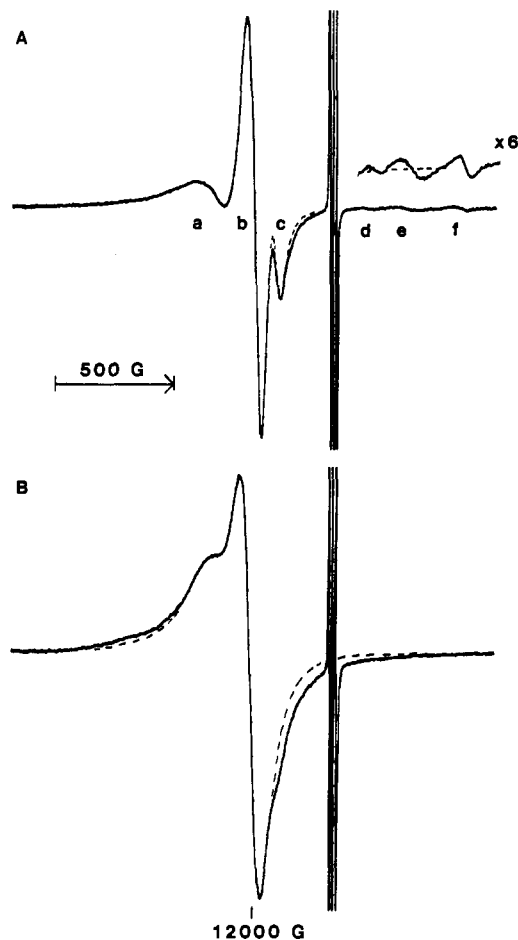
Figure 1. Q-Band EPR spectra (2000 G) of Cu(hfac)$_2$·L at 22 °C: (A) spectrum for L = VIII obtained with 12-mW microwave power and 2-G modulation amplitude; (B) spectrum for L = IX obtained with 12-mW microwave power and 4-G modulation amplitude. The off-scale three-line signals are due to a small amount of spin-labeled ligand that is not bound to Cu(hfac)$_2$. The dashed lines denote the simulations in regions where the simulated spectra do not coincide with the experimental curves.

populations of the species that give these AB patterns are less than about 2%.

Isomers of VIII could be due to cis–trans isomerism about the olefinic bond or rotamers with respect to the single bond between the double bond and the nitroxyl ring. Combination of the two effects could give rise to four species, as observed in the EPR spectra. On the basis of the ^{1}H NMR data for VIII (discussed above), the two major components in the spectrum in Figure 1A (peaks a, b, c, and f) are assigned to isomers with a trans conformation of the olefin. The two minor components (peaks d and e) are assigned to isomers with a cis conformation of the olefin or rotamers with trans olefin.

The second site for isomerism in the complexes of VIII is the central bond of the diene. The barrier to rotation around the central bond in 1,3-butadiene is about 4.0 kcal/mol.[26] The separations between peaks d or e and f (Figure 1A) are sufficiently large that the absence of dynamic averaging at room temperature only requires an activation energy greater than about 5 kcal/mol. The bulky substituents in VIII may cause the barrier to rotation about the central bond of this diene to be greater than in 1,3-butadiene. However, much higher barriers would be required to prevent averaging on the NMR time scale. Thus, it is plausible that these conformers would be averaged in the NMR spectra but not in the EPR spectra. In 1,3-butadiene the population of the trans isomer is about 100 times the population of the minor isomer,[27] which is thought to be a skew or bent conformation rather

(24) Boymel, P. M.; Eaton, G. R.; Eaton, S. S. *Inorg. Chem.* **1980**, *19*, 727.
(25) Reibenspies, J. H.; Anderson, O. P.; Eaton, S. S.; More, K. M.; Eaton, G. R. *Inorg. Chem.* **1987**, *26*, 132.

(26) Squillacote, M. E.; Sheridan, R. S.; Chapman, O. L.; Anet, F. A. L. *J. Am. Chem. Soc.* **1979**, *101*, 3657.
(27) Mui, P. W.; Grunwald, E. *J. Am. Chem. Soc.* **1982**, *104*, 6562.

than cis.[28] Although the trans isomer is likely to be favored for VIII, the ratio of trans to skew is likely to be smaller for VIII than for 1,3-butadiene due to steric interaction between the 2,2-dimethyl protons of the nitroxyl ring and the olefinic proton in the trans isomer. It seems plausible that the major isomer of VIII is trans olefin with a trans conformation of the central bond of the diolefin. The value of J for this isomer is larger than for the other isomers. The fully trans linkage is expected to optimize both the σ and π contributions to the exchange interaction because the σ contribution is greatest through a "W-plan" geometry[29] and the π contribution is greatest for the planar conjugated conformation. It is proposed that the next most abundant isomer (peaks c and f in Figure 1A) is a trans olefin with a skew geometry with respect to the central bond of the diolefin. These assignments would give a trans to skew ratio for VIII of about 5. The value of J for the skew conformation is less than the value for the fully trans conformation by about a factor of 2.5, due to the less favorable geometry for both σ and π interaction.

At Q-band the spectrum of $Cu(hfac)_2 \cdot IX$ (Figure 1B) showed partially resolved peaks for the copper and nitroxyl inner lines, which permitted a determination of $J = 0.25$ cm^{-1}. The discrepancy between the calculated and observed spectra on the high-field side of the nitroxyl inner peak indicates the presence of one or more conformations with $J < 0.25$ cm^{-1}, but the contributions to the spectra were not sufficiently well resolved to define the abundance or values of J for these species.

The two spectra in Figure 1 indicate the utility of Q-band spectra for the determination of J values in the range 0.18–0.25 cm^{-1} for spin-labeled $Cu(hfac)_2$ complexes. When J is less than about 0.050 cm^{-1}, as in the $Cu(hfac)_2$ complexes of I–VII, the values of J are as readily obtained from X-band spectra as from Q-band spectra since the outer lines are sufficiently intense at X-band to permit facile observation. In some cases the line widths of the signals are greater at Q-band than at X-band, which decreases the resolution of the spectra and makes it harder to resolve contributions from multiple species with similar small values of J at Q-band than at X-band. The values of J for $Cu(hfac)_2 \cdot L$, $L = I$–VII, were obtained from the X-band spectra.

The EPR spectra of $Cu(hfac)_2 \cdot L$, $L = III$, IV, VI, and VII, were temperature dependent. At room temperature the nitroxyl signal for $Cu(hfac)_2 \cdot IV$ was a broadened three-line spectrum (Figure 2A). Below 0 °C the spectrum split into two doublets of nitroxyl triplets with values of J that differed by about a factor of 10 (Figure 2B). The isomer with the smaller value of J had the greater abundance and dominated the frozen-solution spectrum. Since the averaged signal at room temperature had a smaller splitting than that observed for either of the slow-exchange signals, the signs of J must be opposite for the two isomers. The room-temperature nitroxyl EPR spectrum for $Cu(hfac)_2 \cdot VI$ was also a broadened triplet and was split into two doublets of nitroxyl triplets below –35 °C. The behavior of $Cu(hfac)_2 \cdot VI$ was similar to that observed for $Cu(hfac)_2 \cdot IV$—the two values of J differed by about a factor of 10, the conformation with the smaller value of J had the greater population, and the signs of J for the two conformations were opposite.

The room-temperature spectra of the nitroxyl signals for $Cu(hfac)_2 \cdot L$, $L = III$, VII, were similar to each other, with a broad doublet of triplets due to $J = 0.0058$ and 0.0080 cm^{-1}, respectively. Below –60 °C the nitroxyl signal for $Cu(hfac)_2 \cdot III$ split into two doublets of triplets with $J = 0.0080$ and 0.0029 cm^{-1}. For $L = VII$ two doublets of triplets with $J = 0.0110$ and 0.0037 cm^{-1} were observed below 10 °C. For these two ligands the isomer with the larger value of J had the greater population and the signs of J are the same for the two isomers.

The barriers to isomerization in $Cu(hfac)_2 \cdot L$, $L = III$, IV, VI, and VII, were estimated to be about 5 kcal/mol by assuming two-site exchange and calculating ΔG^* from the coalescence
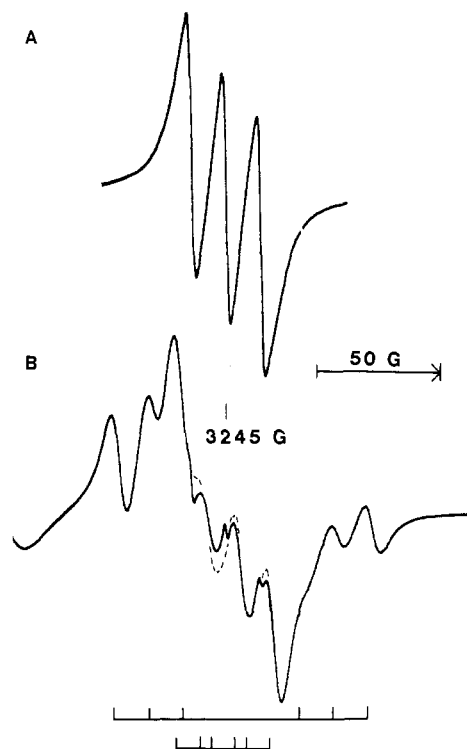
Figure 2. X-Band EPR spectra of the nitroxyl signal obtained when ligand IV is bound to $Cu(hfac)_2$ in toluene solution: (A) 100-G scan at 22 °C obtained with 5-mW microwave power and 0.125-G modulation amplitude; (B) 200-G scan at –40 °C obtained with 5-mW microwave power and 0.63-G modulation amplitude. The stick diagram indicates the contributions from the two isomers to the spectrum in part B. The dashed lines denote the simulations in regions where the simulated spectrum does not coincide with the experimental curve.

temperature and the average separation between the interchanging nitroxyl signals.[30] The values were slightly higher for $L = III$ and VII than for $L = IV$ and VII. It is proposed that this is the barrier to rotation about one of the single bonds in the pyridine–nitroxyl linkage. Ligands III–VII have a carbonyl group in the pyridine–nitroxyl linkage in addition to the olefin in VIII. In III, IV, and VI the carbonyl group is between the olefin and the pyridine ring. Isomers in this system could be due to slowing of rotation about the bond between the two double bonds or the bond between the olefin and the carbonyl. In VII the carbonyl group is adjacent to the nitroxyl ring instead of adjacent to the pyridine ring. In this case there is not a diolefin, so isomerism must be due to slow rotation about the bond(s) to the carbonyl carbon. Since similar barriers to rotation were observed for coordinated VII and III, IV, and VI, it is likely that it is the α-keto linkage that exhibits the isomerism. Alternatively, the barriers to rotation about the bond between the two double bonds and the barrier to rotation of the α-keto linkage may be too similar to distinguish between the two processes in these experiments. The barrier to rotation about the bond between the double bond and the carbonyl group in an acrylic ester was observed to be 6.3 kcal/mol,[31] which is similar to the barriers observed here.

In V the substituent is on the 2-position of the pyridine ring, which causes substantial steric hindrance to coordination. V formed complexes with the four-coordinate $Cu(hfac)_2$ but not with the other metals examined.

Cobalt(II) Complexes. In approximately equimolar solutions, spin-labeled pyridines bind to Co(II) porphyrins to form predominantly $Co(P) \cdot L$.[12] A small amount of dimer is also formed, in which a pyridine nitrogen binds to one Co(P) and the nitroxyl oxygen of the same ligand binds to a second Co(P). The anti-

(28) Breulet, J.; Lee, T. J.; Schaefer, H. F. *J. Am. Chem. Soc.* **1984**, *106*, 6250.

(29) Barfield, M.; Chakrabarti, B. *Chem. Rev.* **1969**, *69*, 759. King, F. W. *Chem. Rev.* **1976**, *76*, 157.

(30) Anet, F. A. L.; Anet, R. In *Dynamic Nuclear Magnetic Resonance Spectroscopy*; Jackson, L. M., Cotton, F. A., Eds.; Academic Press: New York, 1975; p 543.

(31) More, K. M.; Eaton, G. R.; Eaton, S. S. *Can. J. Chem.* **1982**, *60*, 1392.
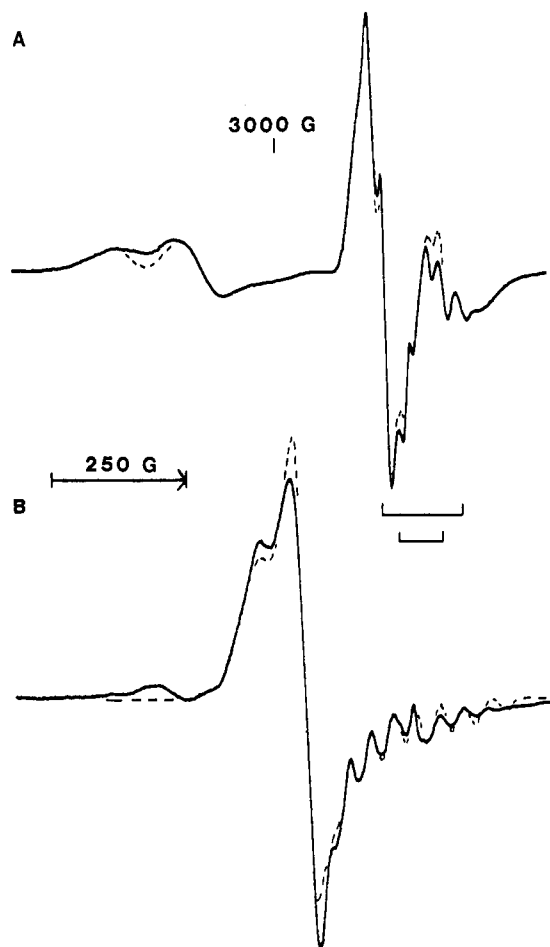
Figure 3. X-Band EPR spectra (1000 G) of Co(P)·L, L = VII (A) and VIII (B), obtained with 4-G modulation amplitude and 1-mW microwave power at −180 °C. The stick diagram in part A highlights the splittings of the nitroxyl signals for the two isomers. The dashed lines denote the simulations in regions where the simulated spectra do not coincide with the experimental curves.

ferromagnetic interaction between Co(II) and the coordinated nitroxyl is sufficiently strong that an EPR signal is not detected for either of the spins. Thus, the EPR spectrum of the dimer is due only to the Co(II) bound to the pyridine nitrogen.

The EPR spectrum of Co(P)·VII is shown in Figure 3A. The low-field doublet is due to splitting of the cobalt perpendicular lines into inner and outer lines. The discrepancy between the calculated and observed signals in this portion of the spectrum is due to the presence of some dimer. It gives cobalt perpendicular lines at the position for Co(P)·py, which is intermediate between the inner and outer cobalt perpendicular lines for the spin-coupled complex. To a first approximation the nitroxyl lines also appear to be split into a doublet. Upon closer inspection it is seen that there are two components of the nitroxyl signal—one with sharper lines and a smaller splitting and a second with broader lines and a larger splitting, as marked in Figure 3A. The two values of J are 0.014 and 0.0095 cm^{-1}. The two components are attributed to the same isomerism that was observed in Cu(hfac)$_2$·VII. Isomers were not detected in the Co(II) complexes of the other spin-labeled ligands. Detection of isomers is more difficult in the Co(II)·L spectra than in the fluid-solution Cu(hfac)$_2$·L spectra. In the frozen-solution spectra, anisotropy causes the signals from a single isomer to be spread over a wider range of magnetic fields than in solution, so overlap of the spectra from multiple species is greater. Even in the spectrum shown in Figure 3A, a small increase in the line widths of the nitroxyl signals easily could have obscured the presence of the two isomers.

In the spectrum of Co(P)·VIII (Figure 3B) the low-field peak that does not appear in the simulation is the cobalt perpendicular lines for the pyridine-bound end of a dimer. The value of J for

Co(P)·VIII is large enough to give lines at the average of the cobalt and nitroxyl g values. The prominent lines in the center of the spectrum are the cobalt and nitroxyl inner lines for molecules in which the magnetic field is in the perpendicular plane of the cobalt axis system. The eight lines toward higher field are inner lines from molecules in which the magnetic field is along the z axis of the cobalt axis system. The eight-line splitting is due to the cobalt nuclear hyperfine interaction ($I = {}^7/_2$), and the splitting constant is half that observed in the absence of electron–electron interaction. The simulated spectrum was obtained with $J = -0.15$ cm^{-1}, an interspin distance of 10 Å, a 30° angle between the cobalt z axis and the interspin vector, and a 90° angle between the cobalt z axis and the nitroxyl z axis. The discrepancy between the calculated and observed spectra indicates that the line widths depend on the cobalt nuclear spin state, which is not included in the calculation.

Vanadyl Complexes. Spin-labeled pyridines bind to VO(hfac)$_2$ to form primarily 1:1 complexes,[4] although there is also some dimer formation. Analogous with the behavior of the corresponding Cu(hfac)$_2$ and Co(P) dimers, the only EPR signal for the dimer is from V^{IV}O bound to the pyridine nitrogen.

In fluid solution at −50 °C, two isomers were observed for VO(hfac)$_2$·L, L = IV and VII but not for L = III, VI, and VIII. Even in the isotropic fluid-solution spectra, it is harder to resolve the contributions from isomers with different values of J for VO(hfac)$_2$·L than for Cu(hfac)$_2$·L. This is due primarily to two factors. Since the vanadium nuclear spin is ${}^7/_2$ and the copper nuclear spin is ${}^3/_2$, there are twice as many metal lines, and therefore twice as many AB patterns in the spin-coupled spectra, for vanadyl as for copper. Secondly, the Cu(hfac)$_2$ g value is sufficiently different from the nitroxyl g value that all of the copper lines in fluid solution occur at lower field than the nitroxyl lines. Thus, all nitroxyl inner lines are at lower field than free nitroxyl, and nitroxyl outer lines are at higher field than free nitroxyl, and there is no overlap of nitroxyl outer lines with copper or nitroxyl inner lines. Ease of observation of the nitroxyl outer lines is particularly useful in determining the value of J since the positions of the outer lines are more sensitive to changes in the value of J than are the inner lines and the nitroxyl outer lines are frequently sharper than the metal outer lines. However, for VO(hfac)$_2$ and nitroxyl, the g-value difference is small enough that at X-band there are four metal lines at higher field and four at lower field than the nitroxyl lines, which causes there to be both nitroxyl inner and nitroxyl outer lines at higher and lower fields than free nitroxyl. Thus, in addition to having twice as many AB patterns for a single isomer in a vanadyl–nitroxyl spectrum as in a copper–nitroxyl spectrum, there is also overlap of inner and outer nitroxyl lines for values of J less than about 0.05 cm^{-1} and overlap of metal and nitroxyl lines. The difficulties in resolving the contributions from two or more isomers are exacerbated if there is a substantial difference in the populations of the isomers. The inability to detect the presence of isomers in some of the vanadyl complexes that would have been expected by analogy with the copper complexes is likely due to the many overlapping lines and may not indicate the absence of isomerism.

Spectra of VO(hfac)$_2$·L at Q-band have the advantage over the X-band spectra that the impact of the g-value difference is increased, which causes only two vanadyl lines to come at lower field and six at higher field than the nitroxyl lines. The resulting separation between the highest field vanadyl line and the nitroxyl signal is about 600 G at Q-band and about 430 G at X-band. Thus, a larger value of J is required to give averaged g and A values at Q-band than at X-band.

The Q-band spectrum of VO(hfac)$_2$·VIII is shown in Figure 4A. The small peak at low field that is not included in the simulations is due to VO(hfac)$_2$ that is not bound to VIII. The sharp off-scale three-line signal is from the unbound ligand VIII. The positions of the vanadyl and nitroxyl inner lines for the AB patterns for each of the eight vanadium nuclear spin states are indicated in the stick diagram below the spectrum. The exchange interaction is strong enough to give average positions for the inner lines of the four AB patterns involving the vanadyl nuclear spin
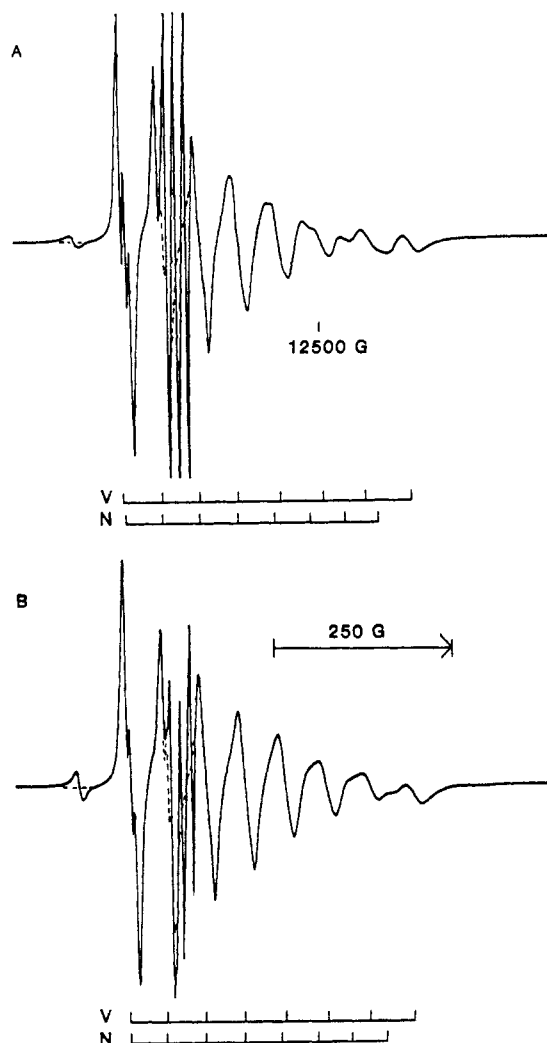
Figure 4. Q-Band EPR spectra (750 G) of VO(hfac)$_2$·L, L = VIII (A) and IX (B), obtained at 22 °C with 1.0-G modulation amplitude and 24-mW microwave power. The stick diagrams below the spectra indicate the positions of the vanadyl (V) and nitroxyl (N) inner lines for the eight vanadyl nuclear spin states. The nitroxyl nitrogen hyperfine splitting is not included in the diagram. The dashed lines denote the simulations in regions where the simulated spectra do not coincide with the experimental curves. The three-line signal at 12 310 G is due to a small amount of spin-labeled ligand that is not bound to VO(hfac)$_2$. The weak low-field line that is not included in the simulations is the $m_I = {}^7/_2$ line for free VO(hfac)$_2$.

states with signals that are closer to the nitroxyl. For the lowest field signal the line widths are sufficiently narrow that the nuclear hyperfine splitting from the nitroxyl nitrogen is resolved. It is reduced to half the value observed in the absence of electron–electron spin interaction. For the four AB patterns involving vanadium nuclear spin states with signals further from the nitroxyl, separate signals are observed for the vanadyl and nitroxyl inner lines. The simulated spectrum was obtained with $J = 0.37$ cm^{-1}.

In the Q-band spectrum of VO(hfac)$_2$·IX (Figure 4B) there was more unbound VO(hfac)$_2$ and less unbound ligand than in the spectrum in Figure 4A. The value of J for VO(hfac)$_2$·IX (0.45 cm^{-1}) is larger than for VO(hfac)$_2$·VIII (0.37 cm^{-1}), so the separation between the vanadyl and nitroxyl inner lines for the AB pattern for a given vanadyl nuclear spin state is smaller in Figure 4B than in Figure 4A.

Chromium Complexes. The equilibrium constant for coordination of spin-labeled pyridines to Cr(TPP)Cl is smaller than for the three other metals in this study, so there was greater interference from the signal from unbound ligand in the spectra of Cr(TPP)Cl·L than in the spectra of complexes for the other metals examined.[23] In addition, the computer program (METNO) used to analyze the spectra for metals with $S > {}^1/_2$ does not include the nitroxyl nitrogen nuclear spin, so simulations could only be
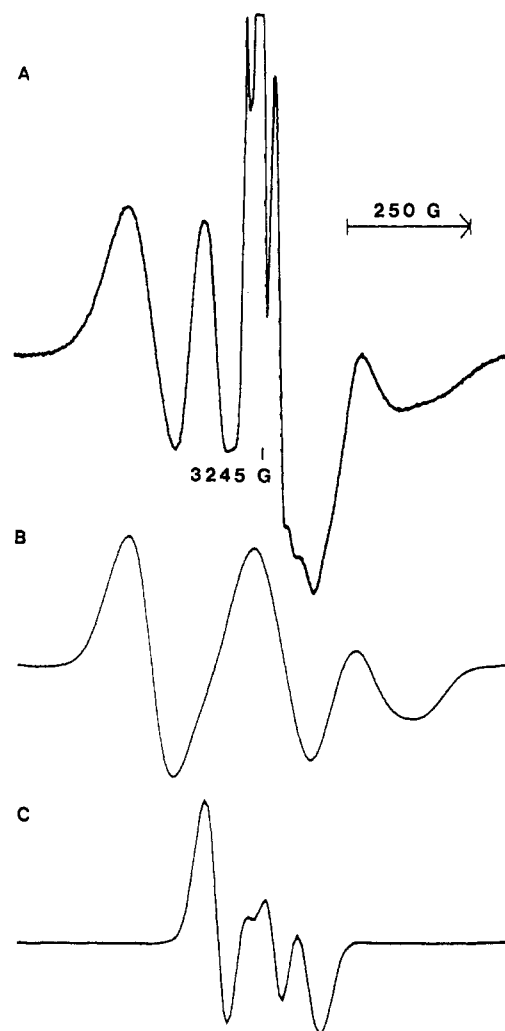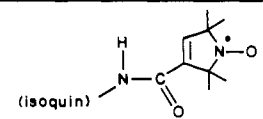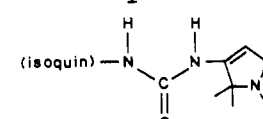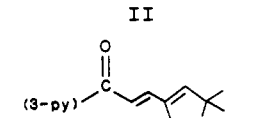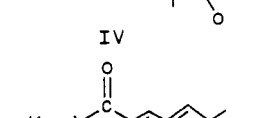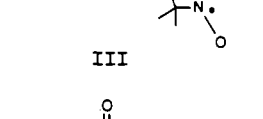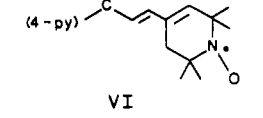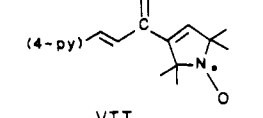

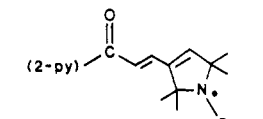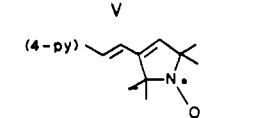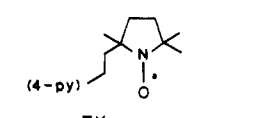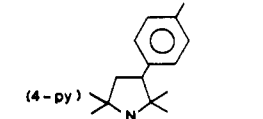**Figure 5.** (A) X-Band EPR spectrum (1000 G) of the nitroxyl signals for Cr(TPP)Cl·VII at −180 °C obtained with 1-mW microwave power and 4-G modulation amplitude. Part of the sharp signal in the center of the spectrum is due to a small amount of VII that is not coordinated. (B) Simulated spectrum for the isomer with $J = 0.017$ cm^{-1}. (C) Simulated spectrum for the isomer with $J = 0.0065$ cm^{-1}.

obtained for complexes in which the value of J was greater than the nitroxyl nitrogen hyperfine splitting. Most of the spectra for Cr(TPP)Cl·L were sufficiently broad that the contributions from isomers could not be resolved.

The central portion of the frozen-solution spectrum of Cr(TPP)Cl·VII is shown in Figure 5A. The signals in this 1000-G scan are predominantly nitroxyl transitions. The turning points in the chromium spectrum occur at higher and lower fields than those shown in Figure 5A. Part of the sharp signal in the center of the spectrum is due to unbound ligand. The spectrum could not be simulated with a single value of J. Figure 5B shows the simulations for one component, obtained with $J = 0.017$ cm^{-1}, an interspin distance of 9.0 Å, and a 25° angle between the interspin vector and the z axis of the chromium zero-field-splitting tensor. The simulation for the second component (Figure 5C) was obtained with $J = 0.0065$ cm^{-1}, an interspin distance of 11 Å, and the interspin vector along the z axis of the chromium zero-field-splitting tensor.

Effect of Metal–Nitroxyl Linkage on J. Isoquinoline Ligands I and II. Comparison of the values of J (Table I) for complexes of these two ligands indicates the relative efficiency of exchange through amide and urea linkages between the isoquinoline ring and the nitroxyl ring. For the Cu(hfac)$_2$ and VO(hfac)$_2$ complexes, exchange was greater through the urea linkage than through the amide linkage, by factors of about 3 and 2, respectively. It was observed previously that exchange interaction was about a factor of 2 greater through urea linkages than through

**Table I.** Values of J $(cm^{-1})^a$ for Transition-Metal Complexes of Spin-Labeled Ligands

| ligand | temp, °C | S = 1/2 | | | S = 3/2 |
		Cu(hfac)$_2$	Co^{II}(P)	VO(hfac)$_2$	Cr(TPP)Cl
I (isoquin)	22	0.0015		0.0044	
	−40	0.0018		0.0046	
	−180	c	b	0.0040	b
II (isoquin)	22	0.0017 (br)		0.0065	
	−40	0.0054		0.0080	
	−180	c	c	c	~0.005
IV (3-py)	22	br		br	
	−40	0.0009, 0.0070 (~3:1)		0.0023, 0.0 (~1:1)	
	−180	b	0.0050	0.0045	b
III (4-py)	22	0.0058		0.0051	
	−60	0.0080, 0.0029, (~3:1)		0.0042	
	−180	c	0.0040	c	~0.005
VI (4-py)	22	br		0.0098	
	−50	0.0005, 0.0050 (~2.5:1)		0.0120	
	−180	<0.0010	0.0060	0.0100	~0.004
VII (4-py)	22	0.0080 (br)		0.0170	
	−40	0.0110, 0.0037 (~3:1)		0.0210, 0.0060 (~3:1)	
	−180	0.019	0.014, 0.0095 (~3:1)	c	0.017, 0.0065 (~3:1)
V (2-py)	22	0.0205			
	−40	0.0195			
	−180	0.016			
VIII (4-py)	22	0.18, 0.075 (~5:1)^d		0.37^d	
	−180	0.18, 0.080	≥0.15	≥0.30	0.15
IX (4-py)	22	0.25^d		0.45^d	
	−180	c	≥0.10	≥0.30	0.12
X (4-py)	22	≥0.15		≥0.20	
	−180	≥0.30	≥0.08	≥0.30	0.27
XI (3-py)	22	≥0.15		≥0.20	
	−180	≥0.30	≥0.08	≥0.30	0.22

^{a} For most of the complexes the sign of J is not known. The uncertainties in the values of J are about ±5% in fluid solution and about ±10% in frozen solution. Spectra were obtained in toluene solution, except that the spectra of the complexes with Cr(TPP)Cl were obtained in 2:1 toluene–chloroform solution. ^{b} The value of J was less than the nitroxyl nitrogen hyperfine splitting. ^{c} These frozen-solution spectra were poorly resolved, presumably due to aggregation of the complex. ^{d} Value of J obtained from Q-band spectra.

amide linkages in compounds with substantial π contributions to the spin delocalization but that exchange was as much as 1 order of magnitude smaller through urea linkages than through amide linkages when the delocalization was predominantly through the σ orbitals.[5,32] Thus, the data for the copper and vanadyl complexes of I and II indicate a substantial π contribution to the electron spin delocalization.

The values of J for the complexes of I and II can also be compared with previously published values for complexes of pyridine derivatives, XV[4] and XVI,[5] which have the same linkages between the aromatic and nitroxyl rings as I and II, respectively.

XV   **XVI**
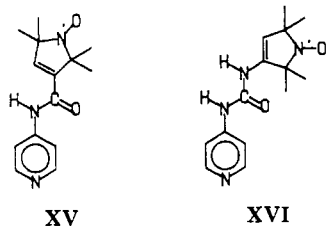
The ratio of the values of J for L = XV and I is 9 for the Cu(hfac)$_2$ complexes and 10 for the VO(hfac)$_2$ complexes. Similarly for the complexes of XVI and II, the ratio of the values of J is 4 for Cu(II), 6 for V^{IV}O, and 7 for Cr(III). To interpret these ratios, differences in both the σ and π contributions to the spin–spin interaction were considered. The bonding pathway through the isoquinoline ring is one carbon longer than through the pyridine ring, which would attenuate the σ contribution to the exchange interaction. This factor is likely to be particularly important for Cu(II) because the copper unpaired electron is in the $d_{x^2-y^2}$ orbital, which has σ symmetry with respect to the orbitals on the coordinated nitrogen. By analogy with the molecular orbitals of naphthalene,[33] both the HOMO and LUMO of isoquinoline have substantial contributions at the 2- and 5-atoms in the ring, which is favorable for the π contribution to the metal–nitroxyl exchange interaction. Thus, the much smaller exchange interaction for the isoquinoline derivatives than for the pyridine derivatives does not appear to be due to unfavorable π distribution in the isoquinoline ring. However, steric interaction between the isoquinoline 5-substituent and the 4-hydrogen prevents coplanarity of the ring and the substituent, which decreases the effectiveness of π delocalization. Although the substituents on the pyridine ring also cannot achieve coplanarity with the ring, the interference is greater for the isoquinoline derivatives than for the pyridine derivatives. This factor is particularly important for the vanadyl complexes because the metal unpaired electron is in the d_{xy} orbital, which has π symmetry with respect to the orbitals on the coordinated ring nitrogen. It appears that both the σ and π contributions to the spin–spin interaction are smaller for the isoquinoline derivatives than for the pyridine derivatives.

Spin-Labeled Pyridines III–VIII. Ligand VIII has an olefinic linkage between the nitroxyl and the pyridine, and ligand XV has an amide linkage, so there are two atoms in the pyridine-nitroxyl linkage for both of these ligands. Since amides usually adopt a trans conformation and the isomers of M·VIII with the larger values of J were assigned (see above) to the trans isomers, comparison of the values of J for these complexes is a measure of the relative effectiveness of exchange interaction through trans olefin and amide linkages. The ratios of the values of J for the complexes of VIII and XV[3] are 11 for Cu(hfac)$_2$, >6 for Co(P), 9 for VO-(hfac)$_2$, and 7 for Cr(TPP)Cl. Thus, the interaction is about 1 order of magnitude greater through the olefin than through the amide and the difference between the two linkages is similar for the four metals. Two factors could contribute to the difference between the amide and the olefin. (1) The olefin and the pyridine ring can be coplanar, but steric interaction between the amide

and the hydrogens on the adjacent carbons of the pyridine ring prevent coplanarity. This decreases the efficiency of π interaction between the pyridine orbitals and the amide orbitals and also prevents a "W-plan" geometry that would optimize σ delocalization. (2) There is less π character in an amide C–N bond than in an olefin C–C bond.

Ligand VII has an α-keto olefin linkage between the pyridine and nitroxyl rings, with the carbonyl group adjacent to the pyrrolinyl-1-oxy ring. Comparison of the values of J for the complexes of VII and VIII indicates the effect of adding a carbonyl group to the metal–nitroxyl linkage. It seems reasonable to compare the larger values of J for each ligand as an indication of the most effective interaction through each type of linkage. As discussed above, the largest value of J probably occurs for the fully trans isomer. The ratios of the values of J for the complexes of VIII and VII were 16 for Cu(hfac)$_2$, >11 for Co(P), 18 for VO(hfac)$_2$, and 9 for Cr(TPP)Cl. This effect is greater than the factor of about 2 decrease observed when a CH$_2$ was added to a linkage with predominantly σ delocalization but less than the factor of ca. 100 decrease observed when a CH$_2$ was added to a linkage with predominantly π delocalization.[5] The magnitude of the change that occurred upon addition of the carbonyl group to the metal–nitroxyl linkage indicates that there was a substantial loss of π delocalization but that the carbonyl group still permitted some π contribution to the metal–nitroxyl interaction.

In ligand III the carbonyl group is added to the pyridine end of the olefinic linkage instead of the nitroxyl end. The bulkiness of the carbonyl group prevents the linkage from being coplanar with the pyridine ring, thereby decreasing the extent of conjugation. The ratio of the values of J for the complexes of VIII and III is 23 for Cu(hfac)$_2$, >38 for Co(P), 72 for VO(hfac)$_2$, and 30 for Cr(TPP)Cl. The larger decrease in J for ligand III compared with VIII than for VII compared with VIII is an indication of the effect of having the α-keto olefin rotated with respect to the plane of the pyridine in addition to the decreased π bonding through the carbonyl carbon.

Ligands III–V have the same α-keto olefin linkage attached at the 2-, 3-, and 4-positions of the pyridine ring. In previous cases where we have examined 2-substituted pyridine spin labels, the substituent contained a coordinating atom and chelation occurred, so the pathways for metal–nitroxyl interaction were different for the 2-isomer than for 3- or 4-isomers.[24,34] The values of J for the chelating 2-isomer were several orders of magnitude greater than for the 3- and 4-isomers. Ligand V does not chelate, but it is so sterically hindered that a significant extent of coordination through the pyridine nitrogen was observed only for Cu(hfac)$_2$. For the copper complexes the values of J decreased in the order 2-isomer (0.0195 cm^{-1}) > 4-isomer (0.0080 cm^{-1}) > 3-isomer (0.0070 cm^{-1}), which indicates that when the 2-isomer is not a chelating ligand, J for the 2-isomer is about the same magnitude as for the 3- and 4-isomers. π delocalization is expected to follow the pattern 2-isomer $\approx$ 4-isomer > 3-isomer, and σ delocalization is expected to give 2-isomer > 3-isomer > 4-isomer.[4] The observed pattern indicates that both σ and π contributions are significant for these Cu(II) complexes. For Co(II) the values of J were 4-isomer (0.0040 cm^{-1}) $\approx$ 3-isomer (0.0050 cm^{-1}), which is consistent with the expectation that spin delocalization is similar for these Co(II) and Cu(II) complexes.[12] However, for the vanadyl complexes the values of J were 4-isomer (0.0042 cm^{-1}) > 3-isomer (0.0023 cm^{-1}), which indicates a greater π contribution to the delocalization for the vanadyl complexes than for the Cu(II) or Co(II) complexes. These patterns parallel prior results.[3,4]

Ligands III and VI differ only the size of the nitroxyl-containing ring. The ratio of the values of J for these ligands was 1.6 for Cu(hfac)$_2$, 1.5 for Co(P), 2 for VO(hfac)$_2$, and 1 for Cr(TPP)Cl. These results are consistent with results on other linkages, which indicated that exchange interaction is slightly larger for the five-membered unsaturated ring nitroxyl than for the six-membered analogue.[4]

(32) More, K. M.; Eaton, G. R.; Eaton S. S. *Inorg. Chem.* **1983**, *22*, 934.
(33) Heilbronner, E.; Bok, H. *The HMO Method and Its Application*; Martin, W., Rackstraw, A. J., Translators; Wiley-Interscience: London, 1970; Vol. 3, p 120.

(34) Boymel, P. M.; Braden, G. A.; Eaton, G. R.; Eaton, S. S. *Inorg. Chem.* **1980**, *19*, 735.

Spin-Labeled Pyridines IX–XI. In these ligands the metal-nitroxyl linkage is via the 2-carbon of the nitroxyl ring, instead of the 3-carbon. The values of J for the complexes of IX were similar to those for complexes of VIII. In IX there is a saturated $(CH_2)_2$ linkage between the 4-position of the pyridine and the 2-carbon of a saturated five-membered-ring nitroxyl. In VIII there is an unsaturated $(CH)_2$ linkage between the 4-position of the pyridine and the 3-carbon of an unsaturated five-membered-ring nitroxyl, which makes the metal–nitroxyl linkage one carbon longer for VIII than for IX. The similarity in the values of J for the complexes of VIII and IX indicates that the nature of the bonding in the metal–nitroxyl linkage is more important than the number of atoms in the linkage—the longer unsaturated linkage is as effective in spin delocalization as the shorter saturated linkage.

The values of J for the complexes of ligands X and XI with $Cu(hfac)_2$, $Co(P)$, and $VO(hfac)_2$ were so large that the metal and nitroxyl inner lines occurred at the average of the metal and nitroxyl g values. As a result, only a lower limit could be placed on the value of J.

Conclusion

The values of J for the isoquinoline complexes were about a factor of 10 smaller than for analogous pyridine derivatives due to decreases in both the σ and π contributions to the interaction. The barrier to rotation about one or more of the single bonds in the pyridine–nitroxyl linkages in III, IV, VI, and VII is about 5 kcal/mol. The differences in the value of J for isomers of the same ligand indicated that the value of J is strongly dependent on the conformation of the metal–nitroxyl linkage. J is about 1 order of magnitude larger for an olefinic linkage than for an amide linkage. Addition of a carbonyl group to the olefinic linkage between the pyridine and the nitroxyl caused a smaller decrease in the value of J when the carbonyl group was adjacent to the pyridine ring (factor of 9–18) than when it was adjacent to the nitroxyl ring (factor of 23–72). When the position of the substituent on the pyridine ring was varied and the 2-isomer could not form a chelate ring, the values of J decreased in the order 2-isomer > 4-isomer > 3-isomer for Cu(II), 4-isomer ≈ 3-isomer for Co(II), and 4-isomer > 3-isomer for vanadyl.

Contribution from the Biomedical Chemistry Research Center, Department of Chemistry, University of Cincinnati, Cincinnati, Ohio 45221-0172

Synthesis and Characterization of Technetium(III) Complexes Containing 2,2′-Bipyridine and 1,10-Phenanthroline. X-ray Crystal Structures of *cis*(*Cl*),*trans*(*P*)-[TcCl₂(P(CH₃)₂C₆H₅)₂(bpy)]B(C₆H₅)₄, *cis*(*Cl*),*trans*(*P*)-[TcCl₂(P(CH₃)₂C₆H₅)₂(phen)]B(C₆H₅)₄, and *cis*(*Cl*),*trans*(*P*)-[TcCl₂(P(CH₃CH₂)(C₆H₅)₂)₂(bpy)]SO₃CF₃[1]

Bruce E. Wilcox,[2] Douglas M. Ho, and Edward Deutsch*

Technetium(III) complexes of the general formula *cis*(*Cl*),*trans*(*P*)-[TcCl₂(P)₂L]⁺, where (P) is dimethylphenylphosphine (PMe₂Ph) or ethyldiphenylphosphine (PEtPh₂) and L is 2,2′-bipyridine (bpy), 4,4′-dimethyl-2,2′-bipyridine (Me₂bpy), or 1,10-phenanthroline (phen), have been synthesized and characterized. They are prepared by L substitution onto, with concomitant displacement of one chloride and one phosphine ligand from, the *mer*-TcCl₃(P)₃ starting material in refluxing ethanol. Analysis of these complexes by fast atom bombardment mass spectrometry (in the positive ion mode) provides "fingerprint" mass spectra that exhibit peaks assigned to the molecular ion M⁺ as well as peaks assigned to M⁺ minus one or more monodentate ligands. Single-crystal X-ray structure determinations of *cis*(*Cl*),*trans*(*P*)-[TcCl₂(PMe₂Ph)₂(bpy)]BPh₄ (A), *cis*(*Cl*),*trans*(*P*)-[TcCl₂(PMe₂Ph)₂(phen)]BPh₄ (B), and *cis*(*Cl*),*trans*(*P*)-[TcCl₂(PEtPh₂)₂(bpy)]SO₃CF₃ (C), with formula weights of 921.62, 945.64, and 903.65, respectively, show that the technetium atoms reside in slightly distorted octahedral environments. Complex A crystallizes in the triclinic space group P1̄, with $a = 10.700$ (2) Å, $b = 14.231$ (2) Å, $c = 16.018$ (2) Å, $\alpha = 95.80$ (1)°, $\beta = 97.58$ (1)°, $\gamma = 108.34$ (1)°, and $V = 2268.5$ (6) Å³, with $Z = 2$ for 3104 observed reflections with $F > 6\sigma(F)$. Complex B crystallizes in the triclinic space group P1̄ with $a = 10.668$ (2) Å, $b = 14.064$ (2) Å, $c = 16.529$ (2) Å, $\alpha = 95.50$ (1)°, $\beta = 97.61$ (1)°, $\gamma = 108.67$ (1)°, and $V = 2309.3$ (7) Å³, with $Z = 2$ for 4975 observed reflections with $F > 3\sigma(F)$. Complex C crystallizes in the orthorhombic space group $P2_12_12_1$ with $a = 16.399$ (2) Å, $b = 21.869$ (5) Å, $c = 11.102$ (2) Å, and $V = 3982$ (1) Å³, with $Z = 4$ for 3585 observed reflections with $F > 6\sigma(F)$.

Introduction

The chemistry and physical properties of polypyridyl complexes containing a wide variety of transition metals have been, and are continuing to be, studied extensively.[3–5] Conspicuously ill represented in this list of metals is technetium. To date, only mono(bipyridine) or -(phenanthroline) complexes of technetium(VII) and technetium(V)[6] and mono- or bis(pyridine) complexes of technetium(IV)[7] have been reported. There are no reports of polypyridyl–technetium complexes in which the technetium center exhibits an oxidation less than +4. This is due in part to the fact that technetium chemistry has only recently begun to be developed[8]

(1) Abstracted from: Wilcox, B. E. Ph.D. Dissertation, University of Cincinnati, 1987.

(2) Current address: Department of Chemistry, Bloomsburg University, Bloomsburg, PA 17815.

(3) (a) Bond, A. M.; Haga, M. *Inorg. Chem.* **1986**, *25*, 4507 and references therein. (b) Ohsawa, Y.; DeArmond, M. K.; Hanck, K. W.; et al. *J. Am. Chem. Soc.* **1983**, *105*, 6522 and references therein. (c) Rillema, D. P.; Taghidiri, D. G.; Jones, D. S.; et al. *Inorg. Chem.* **1987**, *26*, 578 and references therein. (d) Stebler, M.; Ludi, A.; Bürgi, H.-B. *Inorg. Chem.* **1986**, *25*, 4743 and references therein. (e) Nord, G. *Comments Inorg. Chem.* **1985**, *74*, 193. (f) Constable, E. C. In *Advances in Inorganic Chemistry and Radiochemistry*; Emeleus, H. J., Sharpe, A. G., Eds.; 1986, Academic Press: New York, p 69.

(4) Caspar, J. V.; Sullivan, B. P.; Meyer, T. J. *Inorg. Chem.* **1984**, *23*, 2104 and references therein.